REPORT DOCUMENTATION PAGE

Form Approved
OMB No. 074-0188

1. AGENCY USE ONLY (Leave blank)	2. REPORT DATE	3. REPORT TYPE AND DATES COVERED
	12 May 2004	Final, 1 October 2002 - 31 December 2003

4. TITLE AND SUBTITLE

Analysis of Statistical Performance Measures

5. FUNDING NUMBERS

N00014-03-01-0077

6. AUTHOR(S)

Dr. Michael D. Zoltowski

7. PERFORMING ORGANIZATION NAME(S) AND ADDRESS(ES)

Purdue University, W. Lafayette, IN 47907

8. PERFORMING ORGANIZATION REPORT NUMBER

Purdue TR-EE-04-7

9. SPONSORING / MONITORING AGENCY NAME(S) AND ADDRESS(ES)

Office of Naval Research
800 North Quincy Street ONR 321
Arlington VA 22217-5660

10. SPONSORING / MONITORING AGENCY REPORT NUMBER

11. SUPPLEMENTARY NOTES

12a. DISTRIBUTION / AVAILABILITY STATEMENT

Distribution Unlimited

13. ABSTRACT *(Maximum 200 Words)*

When only a limited number of snapshots is available for estimating the spatial correlation matrix, a low-rank solution of the MVDR equations, obtained via a small number of iterations of Conjugate Gradients (CG), can yield a higher SINR than the full-rank MVDR beamformer. A primary issue addressed in this effort is whether the unity gain constraint in the look direction should be enforced a-priori via the use of a blocking matrix, constituting Steering Dependent Conjugate Gradients (SD-CG), or effected a-posteriori through simple scaling of the beamforming vector, constituting Steering Independent Conjugate Gradients (SI-CG). A major contribution was that the two methods yield exactly the same low-rank beamformer. This is an important result since the construction, and application to the data, of a blocking matrix for each "look" direction is computationally burdensome. A simplified expression for the power estimate obtained with the SI-CG beamformer was also developed. Extensive simulations were conducted to verify the efficacy of the theory. While it was known that the optimal number of steps of SI-CG varies with look direction, simulations presented here reveal that the optimal number of principal eigenvectors for the PCI beamformer varies substantially with look direction.

14. SUBJECT TERMS	15. NUMBER OF PAGES
passive sonar, conjugate gradients, adaptive beamforming, reduced-rank filtering	12
	16. PRICE CODE

17. SECURITY CLASSIFICATION OF REPORT	18. SECURITY CLASSIFICATION OF THIS PAGE	19. SECURITY CLASSIFICATION OF ABSTRACT	20. LIMITATION OF ABSTRACT
UNCLASSIFIED	UNCLASSIFIED	UNCLASSIFIED	UL

NSN 7540-01-280-5500

Standard Form 298 (Rev. 2-89)
Prescribed by ANSI Std. Z39-18
298-102

PROJECT TITLE:

ANALYSIS OF STATISTICAL PERFORMANCE MEASURES

PI: Michael D. Zoltowski, Purdue University

FINAL TECHNICAL REPORT: OFFICE OF NAVAL RESEARCH

CONTRACT NUMBER: N00014-03-01-0077
PERFORMANCE PERIOD: 1 October 2002 - 31 December 2003

Principal Investigator:

Michael D. Zoltowski
University Faculty Scholar
School of Electrical Engineering

1285 Electrical Engineering Building
Purdue University
West Lafayette, IN 47907 USA
e-mail: mikedz@ecn.purdue.edu
Phone: 765-494-3512
FAX: 765-494-3512

Program Director:

Dr. John Tague
Team Leader and Program Manager
Office of Naval Research - ONR 321 (US)
Fundamental Research Initiatives Program
Undersea Signal Processing
800 North Quincy Street
Ballston Towers, Tower One
Arlington VA 22217-5660
e-mail: taguej@onr.navy.mil
Phone: 703-696-4399
FAX: 703-696-8423

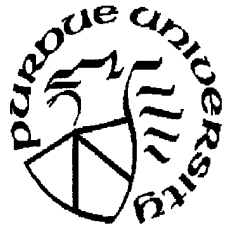

LONG-TERM GOALS

The primary goal of this project is to substantially reduce the computational complexity of the adaptive beamformer employed in real-time passive sonar systems for underwater surveillance. The main methodology for achieving this computational reduction is reduced-rank adaptive filtering via the method of Conjugate Gradients. Reduced-rank adaptive filtering is vitally important for underwater surveillance due to the large number of hydrophones typically employed, coupled with issues of sample support related to target mobility and the high degree of nonstationarity of the underwater environment. The Dominant Mode Rejection (DMR) algorithm is also under investigation for its efficacy in combating the pejorative effects of low sample support.

EXECUTIVE SUMMARY

A key focus of this one year effort involved assessing the efficacy of Signal-Independent Adaptive Beamforming versus Signal-Dependent Adaptive Beamforming (ABF). The scenario assumes the formation of multiple adaptive beams, each pointed to a different "look" direction. For a linear array of N sensors, somewhere between $3N$ and $4N$ adaptive beams are formed encompassing end-fire to end-fire. In Signal-Dependent ABF, a Generalized Sidelobe Canceler (GSC) is formed for each "look" direction. Mathematically, the GSC serves to convert the constrained (quadratic) MVDR optimization problem to an unconstrained optimization problem. From an implementation point of view, the GSC essentially forces adaptation to occur in a subspace orthogonal to the steering vector for the particular "look" direction. This ostensibly serves to prevent "desired" signal cancellation, especially in cases of moderate to low sample support. Implementation of the GSC at each "look" direction requires the construction and application to the data of a blocking matrix for each "look" direction. The attendant computational complexity is substantial. Methods for reducing this complexity for both CG and DMR were the focus of this past year's effort.

When only a limited number of snapshots is available for estimating the spatial correlation matrix, a low-rank solution of the MVDR equations, obtained via a small number of iterations of Conjugate Gradients (CG), can yield a higher SINR than the full-rank MVDR beamformer. A primary issue addressed in this effort is whether the unity gain constraint in the look direction should be enforced a-priori via the use of a blocking matrix, constituting Steering Dependent Conjugate Gradients (SD-CG), or effected a-posteriori through simple scaling of the beamforming vector, constituting Steering Independent Conjugate Gradients (SI-CG). A major contribution was that the two methods yield exactly the same low-rank beamformer. This is an important result since the construction, and application to the data, of a blocking matrix for each "look" direction represents a very substantial computational burden. A simplified expression for the power estimate obtained with the SI-CG beamformer was also developed. Extensive simulations were conducted to verify the efficacy of the theory. While it is previously known that the optimal number of steps of SI-CG varies with look direction, simulations presented here reveal that the optimal number of principal eigenvectors for the PCI beamformer varies substantially with look direction. Simulations also indicate that the SI-CG compared with PCI presents smoother SINR curves as a function of rank implying in less degradation of the SINR if the optimal rank is not chosen. The SI-CG curves also presented slightly higher SINR peaks than the PCI.

APPROACH

When only a limited number of snapshots is available for estimating the spatial correlation matrix, a low-rank solution of the MVDR equations can yield a higher SINR than the full-rank MVDR beamformer. There are several methods of computing low rank MVDR beamformers, e.g., Principal Component Inverse (PCI) , Dominant Mode Rejection (DMR), and the Multi-Stage Wiener Filter (MWF) of Goldstein et al. We previously proved an equivalence between MWF and Conjugate Gradients (CG).

The relationship between Steering-Independent Adaptive Beamforming and Steering-Dependent

Adaptive Beamforming (ABF) was also investigated. The scenario assumes the formation of multiple adaptive beams, each pointed to a different "look" direction. In Steering-Dependent ABF, a Generalized Sidelobe Canceler (GSC) is formed for each "look" direction. Mathematically, the GSC serves to convert the constrained MVDR optimization problem to an unconstrained optimization problem, thereby enforcing a-priori the unity gain constraint in the "look" direction. In contrast, in Steering-Independent ABF, a scaled version of the Wiener-Hopf equations is solved, and the unity gain constraint is enforced a-posteriori through simple scaling of the resulting ABF weight vector.

Implementation of a GSC for each "look" direction requires the construction and application to the data of a blocking matrix for each "look" direction. The attendant computational complexity is quite substantial. In this paper, we prove a very important and somewhat surprising result: the low-rank beamformer obtained with Steering Dependent Conjugate Gradients (SD-CG) is exactly the same as the low-rank beamformer obtained with Steering Independent Conjugate Gradients (SI-CG). Thus, the performance of SD-CG can be obtained without having to form blocking matrices for each "look" direction!

Through simulation results we showed that the optimal rank of the PCI beamformer is a function of the "look" direction. In current practice, the PCI method is applied employing all the dominant eigenvectors of the correlation matrix, which of course does not depend on the look direction and therefore cannot contemplate all "look" directions with an optimal SINR. In the simulations we show that the SINR can undergo expressive variations depending on the rank which is chosen. In the simulations we show that a significant degradation of the SINR occurs if a sub-optimal rank is selected. In addition we observed that the SINR curves using the SI-CG beamformer are much smoother than using the PCI beamformer, much less erratic and they tend to peak a little higher and at a lower rank.

WORK COMPLETED

A key discovery made during the past year effort is that Signal-Independent CG yields the exact same performance as Signal-Dependent CG. This claim is substantiated in the illustrative simulations presented in the next section entitled **Results**. Indeed, the equivalence was first observed in simulations, and then subsequently proven mathematically. This is a very important discovery as it dictates that there is no explicit need for a blocking matrix; this represents a huge savings in computation in terms of avoiding both the construction of the blocking matrix and the application of the blocking matrix to the data. Heretofore, it was thought that both were necessary in order to avoid desired signal cancellation, especially in cases of moderate to low sample support. It turns out that the operation of a blocking matrix is implicitly effected as CG is iterated.

It was also thought that the blocking matrix approach was necessary to obtain an accurate reading on the power at a given source direction, since it explicitly enforces a-priori the constraint of unity gain in the "look" direction. Another very important discovery made during the past year is that once the reduced-rank ABF weight vector is obtained at terminal step K of CG, the power in the corresponding "look" direction may be simply estimated as the reciprocal of the inner product between the ABF weight vector and the steering vector for that "look" direction. That is, we have mathematically proved that this simple calculation yields *exactly* the same power estimate as that obtained with Signal-Dependent CG wherein the blocking matrix is used to enforce the unity gain constraint a-posteriori. Due to the aforementioned equivalence, it also yields the same exact power estimate as Signal-Independent CG, wherein the unity gain constraint is enforced by a-posteriori scaling of the ABF weight vector obtained at terminal step K. Prior to this discovery, the power obtained with a given ABF weight vector was estimated by computing a quadratic form involving the multiplication of the sample correlation matrix with the ABF weight vector. Thus, this second key discovery represents another major reduction in the computational complexity of CG based reduced-rank ABF.

This is in contrast to DMR where for each "look" direction, computing the ABF weight vector involves computing the inner product between each dominant eigenvector and the steering vector for that "look" direction. Again, CG directly outputs the ABF weight vector (no further computation

needed), and the power in the corresponding "look" direction is simply estimated as the reciprocal of the inner product between the ABF weight vector and the steering vector for that "look" direction.

We also mathematically proved that if there are K sources in the array data, only K+1 steps of CG are needed to obtained the best SINR, if you have an ideal correlation matrix and white noise; taking additional CG teps yields the same ABF vector. This result has theoretical implications with respect to convergence. Note, though, it often takes substantially less than K+1 steps to obtain the "best" performance with either moderate to low sample support. Other key accomplishments during the past one year effort are related in the next section entitled **Results**.

RESULTS

Simulations were conducted employing a linear array of $M = 24$ elements with half-wavelength spacing. The noise was spatially and temporally white Gausian. Two scenarios were used in the simulations. In the first scenario there were 17 incident signals with the arrival angle directions and respective SNRs (as ordered pairs): $(-70°, 23)$;
$(-51°, 12); (-47°, 20); (-41°, 20); (-35°, 29); (-27°, 25)$;
$(-26°, 13); (-19°, 23); (0°, 10); (6.8°, 30); (12°, 29)$;
$(20°, 22); (24°, 11); (24°, 23); (38°, 14); (48°, 22); (87°, 11)$.
For this scenario Figs. 1 to 3 illustrate the directions of the signals as well as the array power pattern for the CBF for the directions of 0°, 6.8° and 14°. At the direction of 0° there is a low SNR signal; at 6.8° there is a high SNR signal and at 14° there is no signal.

In the second scenario there were also 17 incident signals with the arrival angle directions and respective SNRs (as ordered pairs): $(-70°, 23)$;
$(-51°, 12); (-47°, 20); (-41°, 20); (-35°, 29); (-27°, 25)$;
$(-26°, 13); (-19°, 23); (5°, 22); (20°, 21); (21°, 30)$;
$(24°, 11); (24°, 23); (38°, 14); (55°, 29); (60°, 10); (87°, 11)$.
For this scenario Figs. 4 to 6 illustrate the directions of the signals as well as the array power pattern for the CBF for the directions of 60°, 55° and 30°. At the direction of 60° there is a low SNR signal; at 55° there is a high SNR signal and at 30° there is no signal.

For scenario 1, Figs. 7 and 8 plot the SINR versus the rank of the beamformer for the signal at 0° for sample supports of $2M$ and $1M$, respectively. The beamformers used were the SI-CG, SD-CG and DMR. There are 2 strong interferes located on the first and second sidelobes of the CBF as shown in Fig. 1, with powers approximately 20 dB above the power of the desired signal. In order to minimize the effect of these interferes ABF is used. It can be observed from the plots that ABF provides a substantial improvement of the SINR over the CBF, i.e. the rank 1 beamformer. For the DMR beamformer the optimal rank is 10 when the sample support is of $2M$ and the optimal rank is 7 when the sample support is of $1M$. For the CG beamformer for both sample supports of $2M$ and $1M$ the optimal rank is 3. For purposes of comparison, the horizontal line indicates the optimal SINR that would be achieved with the MVDR beamformer computed from the true (ideal) correlation matrix.

Figs. 9 and 10 plot the SINR for the high SNR signal at 6.8°, also for sample supports of $2M$ and $1M$, respectively. Even though there is a interferent signal in the first sidelobe of the CBF (see Fig. 2); the CBF is the beamformer that yields the higher SINR. This because the power of this interferent signal is 20 dB below the desired signal and the low sample support of the correlation matrix is insufficient for a gain using ABF. The CBF is the best beamformer for both sample supports of $2M$ and $1M$. The the SINR degrades for higher rank beamformers. These examples show that the best rank depends on the look direction and on the sample support of the correlation matrix. This stresses the importance of selecting the optimal rank. Fig. 9 reveals that when using the DMR beamformer there can be a difference of 30 dB in the output SINR, depending on which rank is selected.

Figs. 11 and 12 plot the estimated power arriving from the direction 14°, also for a sample support of $2M$ and $1M$, respectively. There is no signal arriving from this direction, therefore the desired

value of the estimated power is the power of the white noise. The horizontal line indicates the output power obtained using a full rank MVDR beamformer with knowledge of the true (ideal) correlation matrix. Ideally, this represents the noise floor. For the sample support of $2M$ the optimal rank of the CG beamformer is 13, while for the sample support of $1M$ the optimal rank is around 10. It is observed that the CG beamformer converges to its minimum power at a significantly lower rank than the DMR beamformer. In general, the optimal number of principal eigenvectors required by the DMR beamformer for non-signal look directions is a large fraction of the number of sensors, M. It is also observed that a sample support level of $2M$ snapshots yields an output minimum power that is closer to the noise floor than that obtained with $1M$ snapshots.

It is observed that SI-CG and SD-CG yield the same SINR at each rank, as expected since it was herein proven that they yield the exact same beamformer. It is also observed that the optimal rank varies with sample support as well as with look direction. While it is well known that the optimal number of steps of CG varies with look direction, it was not heretofore known that the optimal number of principal eigenvectors for the DMR beamformer varies substantially with look direction.

For scenario 2, Figs. 13 and 14 plot the SINR versus rank for the low SNR signal at 60° for sample supports of $2M$ and $1M$, respectively. As shown in Fig. 4 there is a strong interferent signal in the main lobe of the CBF with a power of 19 dB above the power of the desired signal. With ABF the effect of this interferent signal can be minimized. The optimal rank of the CG beamformer is 6 for both sample supports of $2M$ and $1M$. For the DMR beamformer the optimal rank is 11 for both sample supports. Because the CBF tends to have a wide mainlobe when it's look direction is close to the extremity of the array, the probability of having a interferent signal within the mainlobe increases.

Figs. 15 and 16 plot the SINR for the high SNR signal at 60° for sample supports of $2M$ and $1M$, respectively. Here also there is a interferent signal in the mainlobe of the CBF. However this signal has a power of 19 dB below the power of the desired signal and therefore the CBF yields the highest SINR for the both sample supports of $2M$ and $1M$.

Figs. 17 and 18 plot the estimated power arriving from the direction 30°, also for sample supports of $2M$ and $1M$, respectively. There is no signal arriving from this direction.

We have observed that if when estimating the covariance matrix we suppress the desired signal then there is a significant gain in the SINR with ABF. For scenario 1, Figs. 19 and 20 plot the SINR versus rank of the beamformer when the desired signal is suppressed from the correlation matrix for the signal arriving at 0° and for sample supports of $2M$ and $1M$, respectively. Comparing with Figs. 7 and 8, where the desired signal is not suppressed from the correlation matrix; we can observe a gain of approximately 3 dB for the $2M$ sample support case and approximately 4 dB for the $1M$ sample support case.

Figs. 21 and 22 plot the SINR when the desired signal is suppressed from the correlation matrix for the signal arriving at 6.8° of scenario 1 and for sample supports of $2M$ and $1M$, respectively. Comparing with Figs. 9 and 10, where the desired signal is not suppressed from the correlation matrix; we can observe a considerable gain in the SINR. Different from Figs. 9 and 10 the CBF is no longer the optimal beamformer and there is a gain of approximately 8 dB in the maximum SINR from Fig. 9 to Fig. 21.

For scenario 2, Figs. 23 and 24 plot the SINR when the desired signal is suppressed from the correlation matrix for the signal arriving at 60° for sample supports of $2M$ and $1M$ respectively. Comparing with Figs. 13 and 14 where the desired signal is not suppressed from the correlation matrix we can also observe a substantial gain in the SINR.

Also, with the desired signal suppressed from the correlation matrix, Figs. 25 and 26 plot the SINR for the signal at 55° for the sample supports of $2M$ and $1M$, respectively. Comparing with Figs. 15 and 16 where the desired signal is not suppressed from the correlation matrix we can also observe a substantial gain in the SINR.

IMPACT/APPLICATIONS

This work will yield substantial reductions in the computational complexity associated with implementing adaptive beamformers in real-time passive sonar systems for underwater surveillance.

- **Take-Aways:**
  - The optimal number of dominant eigenvectors for SI-PCI (DMR) varies substantially from beam to beam; using the same number of dominant eigenvectors for each "look" direction in DMR is highly sub-optimal.
  - Fig. 1(b) reveals that DMR should only use a single eigenvector for a source direction corresponding to a moderately strong signal arrival, else the error in estimated power for that direction can be as much as 30 dB.
  - Figures 1(c) and 1(d) reveal that a large number (15) of dominant eigenvectors for SI-PCI (DMR) are needed for non-source directions, else Fig. 1(d) reveals that the estimated signal power can be off from the noise floor by over 20 dB (false alarms.)
  - The optimal number of CG steps is significantly less than optimal number of dominant eigenvectors for SI-PCI (DMR), for both source and non-source directions, implying CG has lower computational complexity.

TRANSITIONS

We continue to inform Dr. Norm Owlsey of research progress on this project and look forward to processing real data from his experimental system in the near future.

RELATED PROJECTS

There is a synergism between this work and research being conducted in parallel for a National Science Foundation project entitled "Reduced-Dimension Decision Feedback Equalizers (DFE's) for 4G High-Speed Wireless Digital Communications." This is a single Principal Investigator grant funded by the Computing and Communications Research Division of the CISE Directorate at NSF. (Grant Number: CCR-0118842. Duration: 1 Sept. 2001 - 31 Aug. 2004.) Equalization of Digital TV is an ideal application for CG based adaptive filtering due to the high dimensionality of the DFE; current receiver chips have 576 DFE taps that need to be adapted with time.

PUBLICATIONS

1. M. D. Zoltowski, "Signal-Dependent reduced-rank multibeam array processing" 2003 Underwater Acoustic Signal Processing Workshop 8-10 October 2003. RI, Conference abstract. ONR Grant No. N00014-03-01-0077.

2. M. D. Zoltowski and E. L. Santos, "Matrix conjugate gradients for the generation of high-resolution spectrograms" 2003 37th Asilomar Conference on Signals, Systems, and Computers, pages 1843-1847. November 9-12, 2003.

3. M. D. Zoltowski and E. L. Santos, "Advances in reduced rank adaptive beamforming" SPIE Defense and Security Symposium 2004, Digital Wireless Communications VI, Orlando, FL, April 12-16. (paper presented and in print.)

4. E. L. Santos and M. D. Zoltowski, "On low rank MVDR beamforming using the conjugate gradient algorithm" ICASSP 2004 IEEE International Conference on Acoustics, Speech and Signal Processing. Montreal, Canada, May 17-21, 2004.

5. E. L. Santos and M. D. Zoltowski, "Adaptive beamforming with low sample support via indirect dominant mode rejection" SAM 2004 Third IEEE Sensor array and multichannel signal processing workshop. July 18-21, 2004. Sitges, Barcelona, Spain. Accepted but not yet published.

6. E. L. Santos and M. D. Zoltowski, "Adaptive beamforming with parametric estimation of the correlation matrix" 2004 IEEE Signal Processing Society 11th Digital Signal Processing Workshop. August 1-4, 2004. Taos Ski Valley, New Mexico.

7. E. L. Santos and M. D. Zoltowski, "Adaptive beamforming with low sample support via parametric estimation of the correlation matrix" MILCOM 2004 Military Communications Conference 2004. Monterey, CA, October 31-November 3, 2004.

1 HONORS/AWARDS

1. I received the **2002 Technical Achievement Award of IEEE Signal Processing Society.** The site http://www.ieee.org/organizations/society/sp/techachv.html posts past recipients and states that "The Technical Achievement Award honors a person who, over a period of years, has made outstanding technical contributions to the theory and/or practice in technical areas within the scope of the Society, as demonstrated by publications, patents, or recognized impact on the field." The award consists of an engraved plaque and $1500.

2. I was elected as a **2003 Distinguished Lecturer for IEEE Signal Processing Society.** The site http://www.ieee.org/organizations/society/sp/dlinfo.html posts the topics that I will lecture on and relates the "The Society's Distinguished Lecturer Program provides means for chapters to have access to individuals who are well known educators and authors in the fields of signal processing, to lecture at Chapter meetings."

3. I was elected **Vice-Chairman** of the **Sensor Array and Multichannel Technical Committee** of the **IEEE Signal Processing Society** for a three year term which commenced 1 January 2003. The current membership of the SAM TC is posted at http://www.engr.uconn.edu/ willett/barney.html#SECTION1

4. I was appointed **Area Editor** for the **IEEE Signal Processing Magazine**, in charge of all feature and tutorial articles for a three year term which commenced 1 May 2002. The Area Editors and current Editorial Board for the IEEE Signal Processing Magazine is posted at http://www.cspl.umd.edu/spm/edboard.html

5. I was appointed to serve on the **Awards Board** of the **IEEE Signal Processing Society** for a three year term starting 1 January 2003.

6. I was selected (by student voting) for the **2002 Wilfred Hesselberth Award for Teaching Excellence**, Purdue University, 23 April 2002. This is the top Teaching Award for the School of Electrical and Computer Engineering (75 faculty). This resulted in a full page citation in the *2001-2002 Teaching Awards, Schools of Engineering* brochure, a plaque, a $2K award, and my named engraved on plaque outside ECE Main Office.

7. I was a Faculty Recipient of a **2002 Eaton Design Award** conferred by Purdue ECE on 8 March 2002. This award recognizes a recent alumnus who has made substantial design contributions in industry, while also recognizing the faculty member, indicated by the alumnus, as having the most impact on their design experience at Purdue. My name is engraved on a plaque outside the ECE Main Office.

8. I was appointed to serve on the **Advisory Council for the Department of Electrical and Computer Engineering at Drexel University.** . Appointment at Alma Mater started August 2002. ***Also*:** a highlight article on my research appeared in Drexel University's (i) 2003 College of Engineering Brochure, (ii) Spring 2003 Electrical and Computer Engineering (ECE) Newsletter, and (iii) Web Page's Alumni News Section.

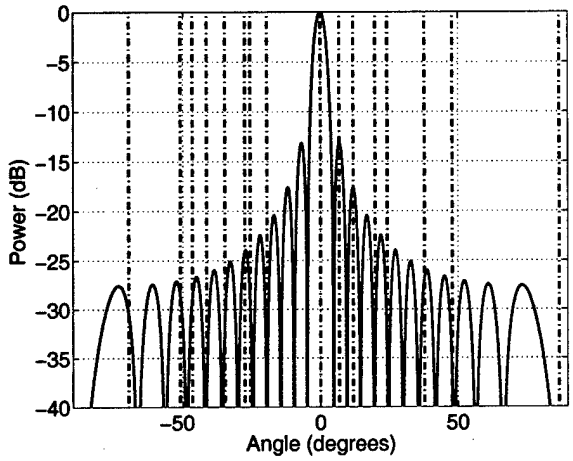

Fig. 1. Scenario 1, array pattern of the CBF for the direction 0° and arriving signals. High power interferent signals in the first and second sidelobes.

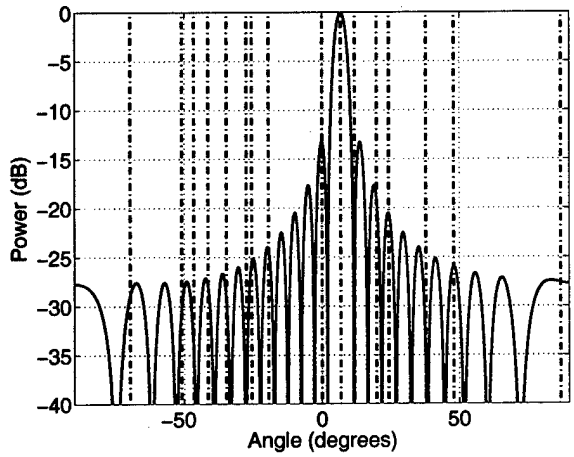

Fig. 2. Scenario 1, array pattern of the CBF for the direction 6.8° and arriving signals. Low power interferent signal in the first sidelobe.

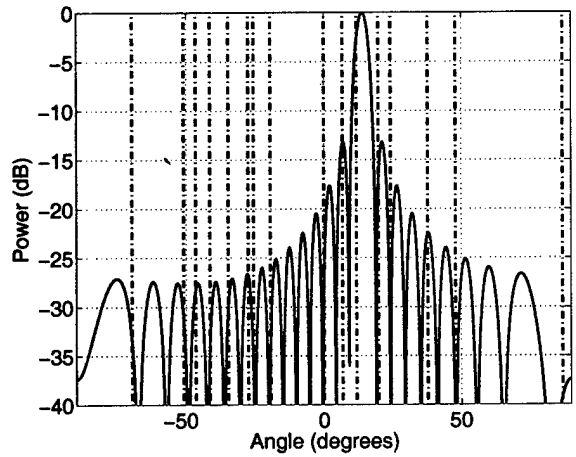

Fig. 3. Scenario 1, array pattern of the CBF for the direction 14° and arriving signals. Direction with no signal.

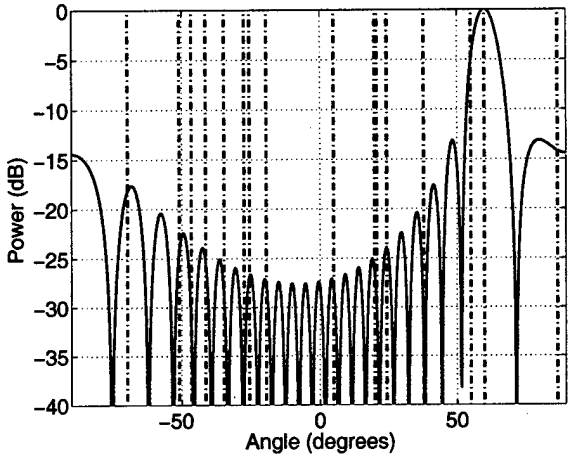

Fig. 4. Scenario 2, array pattern of the CBF for the direction 60° and arriving signals. High power interferent signal in the mainlobe.

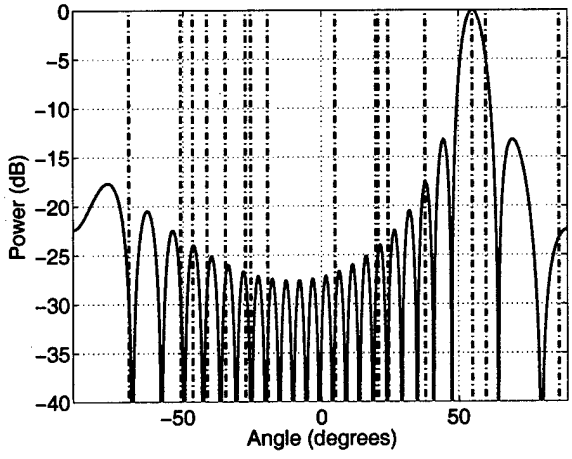

Fig. 5. Scenario 2, array pattern of the CBF for the direction 55° and arriving signals. Low power interferent signal in the mainlobe.

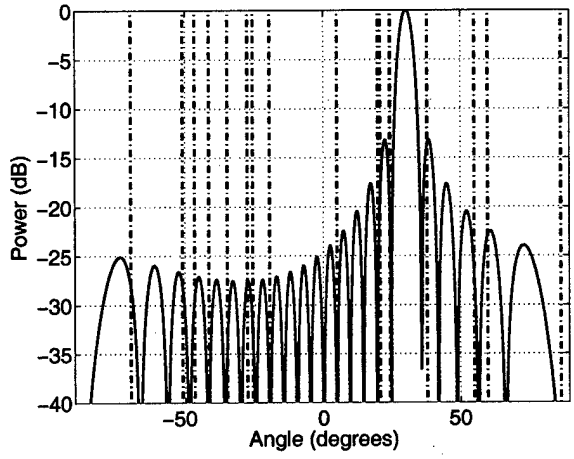

Fig. 6. Scenario 2, array pattern of the CBF for the direction 30° and arriving signals. Direction with no signal.

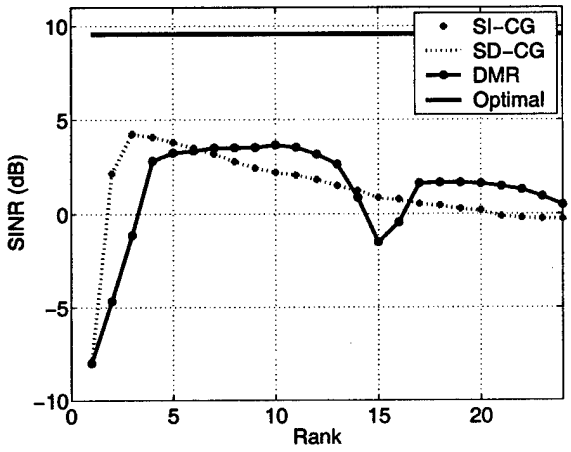

Fig. 7. SINR performance for signal at 0°, $2M$ snapshots, scenario 1. High power interferent signals in the first and second sidelobes of the CBF.

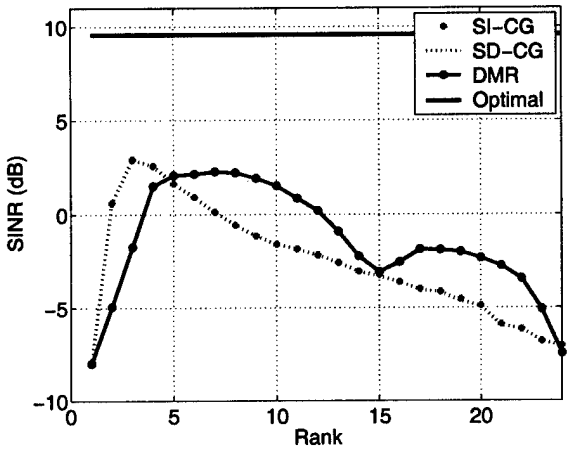

Fig. 8. SINR performance for signal at 0°, $1M$ snapshots, scenario 1. High power interferent signals in the first and second sidelobes of the CBF.

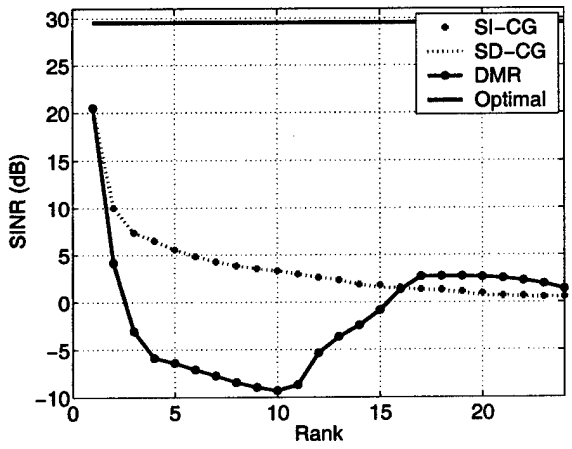

Fig. 9. SINR performance for signal at 6.8°, $2M$ snapshots, scenario 1. Low power interferent signals in the first sidelobe.

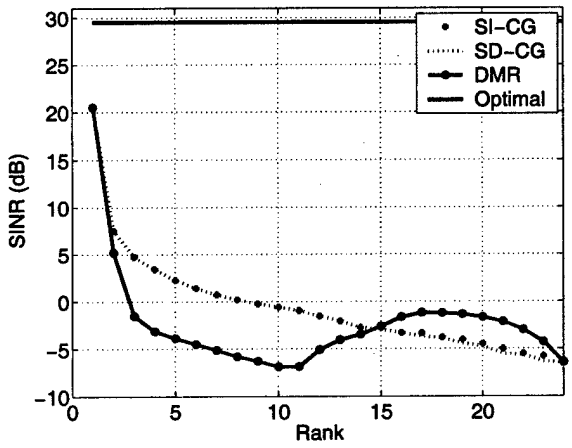

Fig. 10. SINR performance for signal at 6.8°, $1M$ snapshots, scenario 1. Low power interferent signals in the first sidelobe.

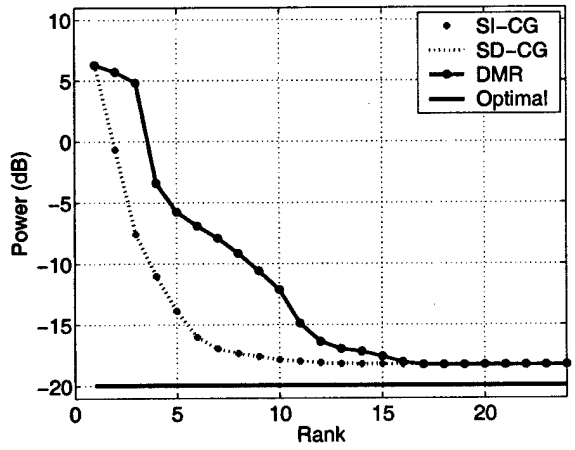

Fig. 11. Power estimation for direction 14°, $2M$ snapshots, scenario 1. Direction with no signal.

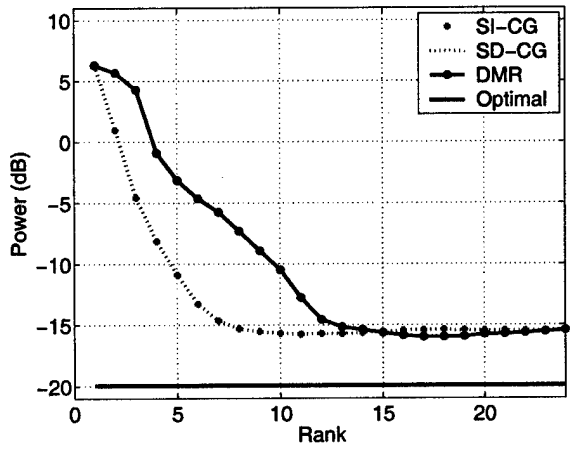

Fig. 12. Power estimation for direction 14°, $1M$ snapshots, scenario 1. Direction with no signal.

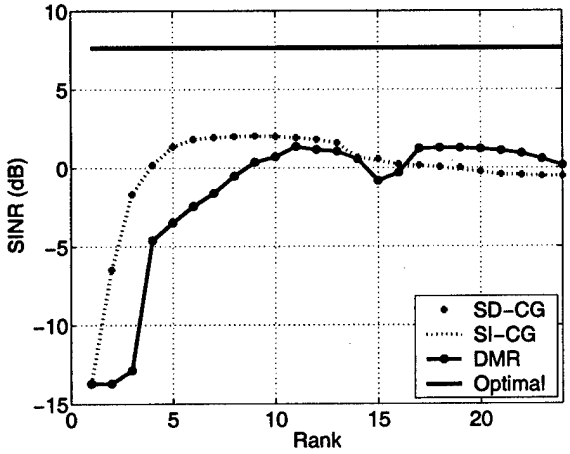

Fig. 13. SINR performance for signal at 60°, $2M$ snapshots, scenario 2. High power interferent signal in the mainlobe.

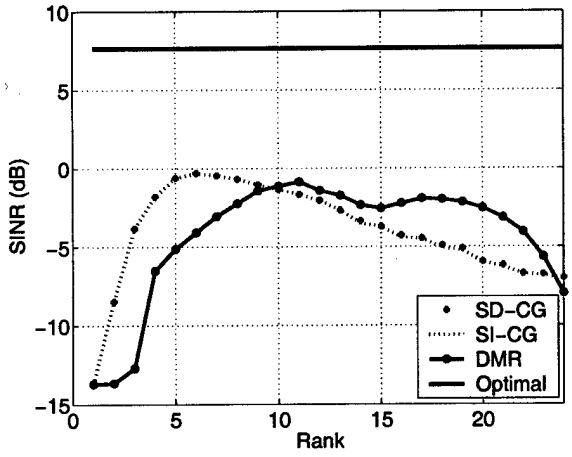

Fig. 14. SINR performance for signal at 0°, $1M$ snapshots, scenario 2. High power interferent signal in the mainlobe.

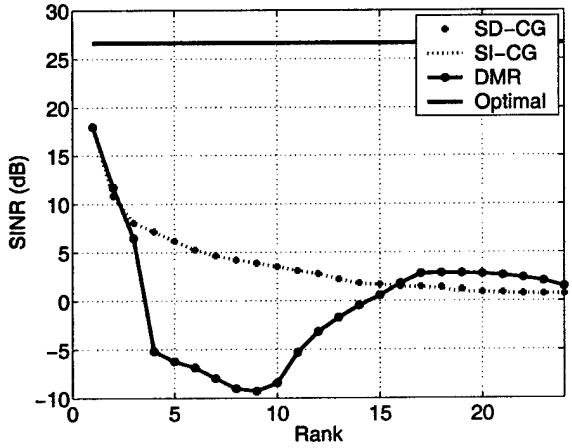

Fig. 15. SINR performance for signal at 55°, $2M$ snapshots, scenario 2. Low power interferent signal in the mainlobe.

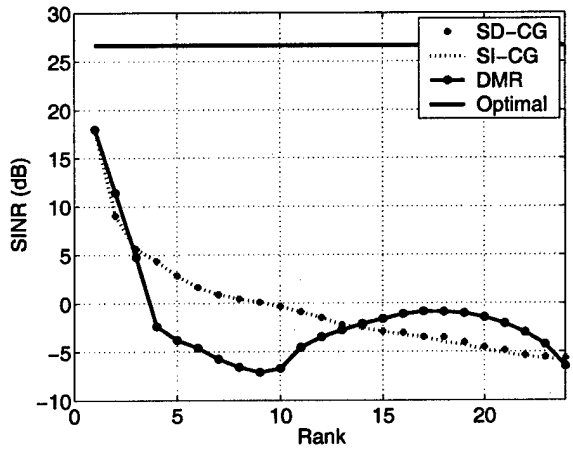

Fig. 16. SINR performance for signal at 55°, $1M$ snapshots, scenario 2. Low power interferent signal in the mainlobe.

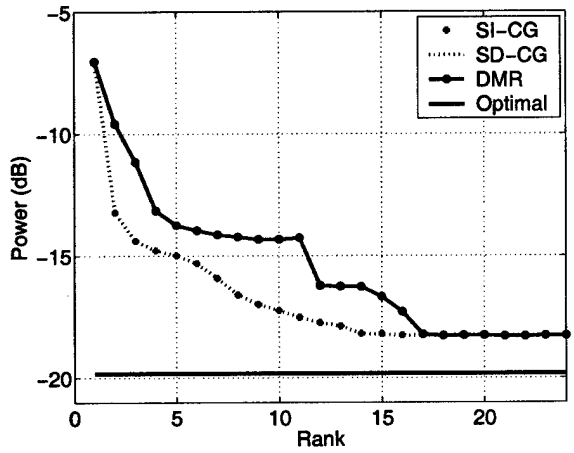

Fig. 17. Power estimation for direction 30°, $2M$ snapshots, scenario 2. Direction with no signal.

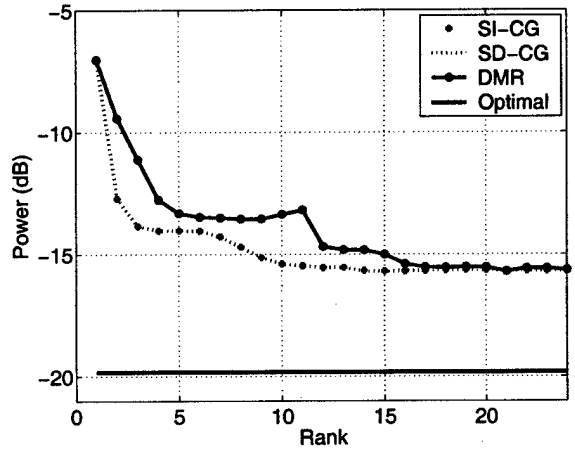

Fig. 18. Power estimation for direction 30°, $1M$ snapshots, scenario 2. Direction with no signal.

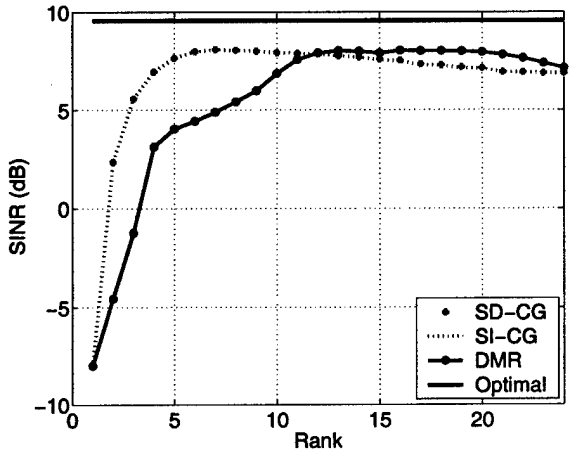

Fig. 19. SINR performance with desired signal suppressed from estimate of correlation matrix for signal at 0°, $2M$ snapshots, scenario 1. Compare with fig. 7.

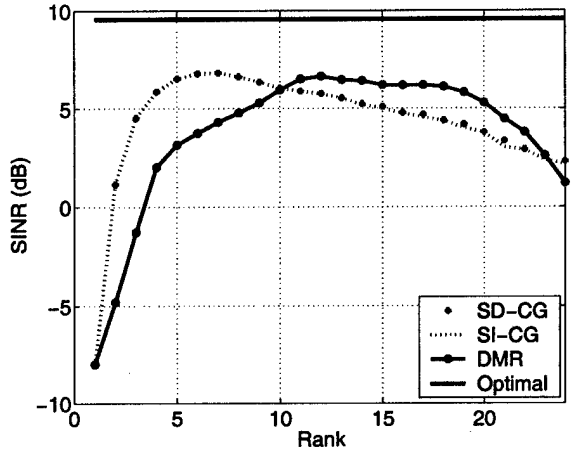

Fig. 20. SINR performance with desired signal suppressed from estimate of correlation matrix for signal at 0°, $1M$ snapshots, scenario 1. Compare with fig. 8.

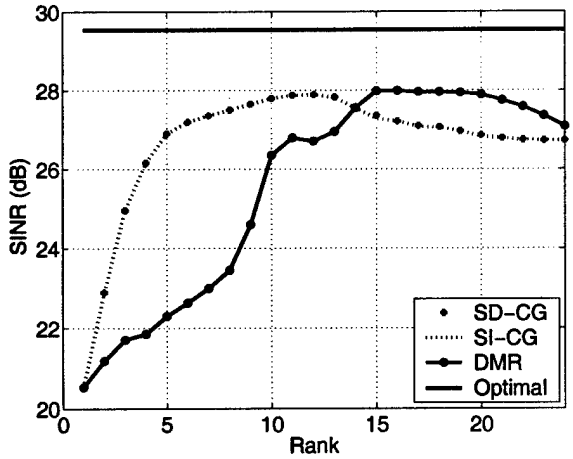

Fig. 21. SINR performance with desired signal suppressed from estimate of correlation matrix for signal at 6.8°, $2M$ snapshots, scenario 1. Compare with fig. 9.

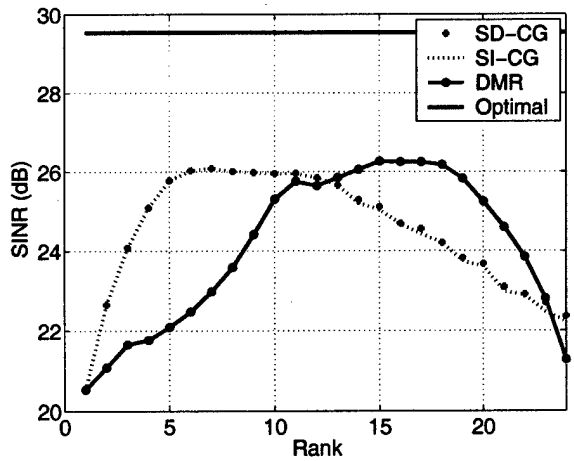

Fig. 22. SINR performance with desired signal suppressed from estimate of correlation matrix for signal at 6.8°, $1M$ snapshots, scenario 1. Compare with fig. 10.

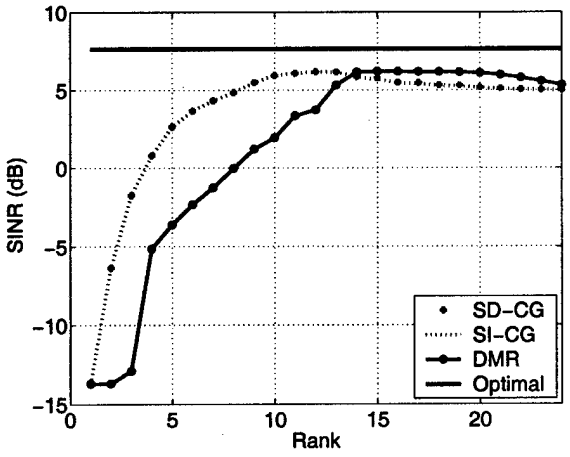

Fig. 23. SINR performance with desired signal suppressed from estimate of correlation matrix for signal at 60°, $2M$ snapshots, scenario 2. Compare with fig. 13.

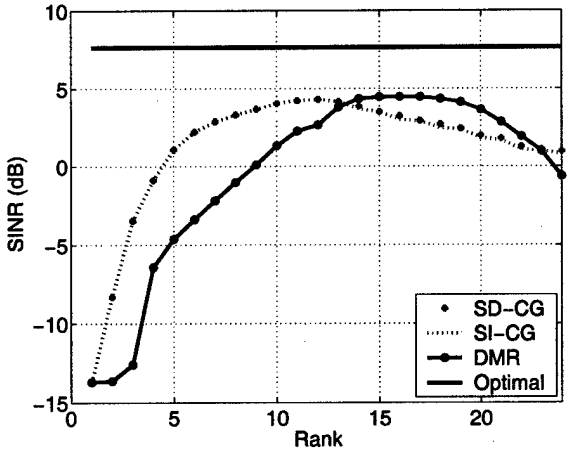

Fig. 24. SINR performance with desired signal suppressed from estimate of correlation matrix for signal at 60°, $1M$ snapshots, scenario 2. Compare with fig. 14.

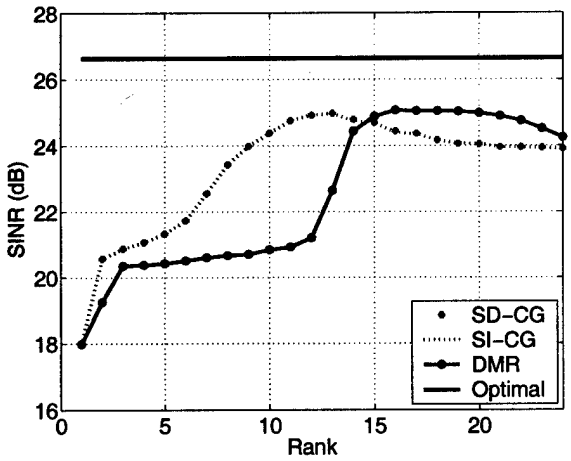

Fig. 25. SINR performance with desired signal suppressed from estimate of correlation matrix for signal at 55°, $2M$ snapshots, scenario 2. Compare with fig. 15.

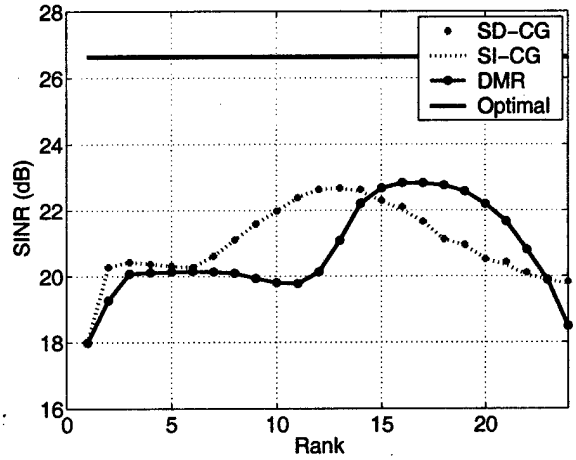

Fig. 26. SINR performance with desired signal suppressed from estimate of correlation matrix for signal at 55°, $1M$ snapshots, scenario 2. Compare with fig. 13.